

## Scanning Electrochemical Microscopy: Surface Interrogation of Adsorbed Hydrogen and the Open Circuit Catalytic Decomposition of Formic Acid at Platinum

Joaquín Rodríguez-López and Allen J. Bard\*

Center for Electrochemistry, Department of Chemistry and Biochemistry, Center for Nano- and Molecular Science and Technology, The University of Texas at Austin, Austin, Texas 78712

Received October 22, 2009; E-mail: ajbard@mail.utexas.edu

**Abstract:** The surface interrogation mode of scanning electrochemical microscopy (SECM) is extended to the *in situ* quantification of adsorbed hydrogen,  $H_{\text{ads}}$ , at polycrystalline platinum. The methodology consists of the production, at an interrogator electrode, of an oxidized species that is able to react with  $H_{\text{ads}}$  on the Pt surface and report the amounts of this adsorbate through the SECM feedback response. The technique is validated by comparison to the electrochemical underpotential deposition (UPD) of hydrogen on Pt. We include an evaluation of electrochemical mediators for their use as oxidizing reporters for adsorbed species at platinum; a notable finding is the ability of tetramethyl-*p*-phenylenediamine (TMPD) to oxidize (interrogate)  $H_{\text{ads}}$  on Pt at low pH (0.5 M  $H_2SO_4$  or 1 M  $HClO_4$ ) and with minimal background effects. As a case study, the decomposition of formic acid (HCOOH) in acidic media at open circuit on Pt was investigated. Our results suggest that formic acid decomposes at the surface of unbiased Pt through a dehydrogenation route to yield  $H_{\text{ads}}$  at the Pt surface. The amount of  $H_{\text{ads}}$  depended on the open circuit potential (OCP) of the Pt electrode at the time of interrogation; at a fixed concentration of HCOOH, a more negative OCP yielded larger amounts of  $H_{\text{ads}}$  until reaching a coulomb limiting coverage close to 1 UPD monolayer of  $H_{\text{ads}}$ . The introduction of oxygen into the cell shifted the OCP to more positive potentials and reduced the quantified  $H_{\text{ads}}$ ; furthermore, the system was shown to be chemically reversible, as several interrogations could be run consecutively and reproducibly regardless of the path taken to reach a given OCP.

### Introduction

We report on the use of scanning electrochemical microscopy (SECM)<sup>1</sup> in the surface interrogation (SI) mode<sup>2</sup> for the detection of adsorbed hydrogen,  $H_{\text{ads}}$ , an oxidizable adsorbate,<sup>3</sup> on a Pt surface. We studied the decomposition of formic acid (HCOOH) in solution on an unbiased Pt surface to produce  $H_{\text{ads}}$ , as a model application of this mode to catalysis. The SECM is an electroanalytical technique that enables the study of chemical and electrochemical aspects of diverse interfaces<sup>1,4,5</sup> and has been used in a variety of modes for the study of catalytic and electrocatalytic processes.<sup>1,6</sup> We recently introduced the SI-SECM for the quantification of an electrogenerated adsorbate, chemisorbed oxygen, on Pt and Au as a function of potential, where the tip interrogated the metal substrate by generating a “titrant” that could reduce the surface oxide species.<sup>2</sup> In the present study, we explore the complementary case of the detection

and quantification of an oxidizable adsorbate by generating an oxidant at the tip. We also elaborate on the use of this mode for the interrogation of the adsorbed products of a heterogeneous catalytic reaction at a substrate, with special emphasis on our ability to do so without the direct participation of the substrate in the analytical process. The technique allows examination of a substrate at open current (OC) and decouples its role as electrocatalytic surface and means of analysis, as is commonly the case in the electrochemical quantification of adsorbed species.<sup>3,7</sup> Such a strategy allows a simple and direct route to determine *in situ* the surface coverage of reaction intermediates and provides insight into species that otherwise remain obscured by side processes occurring at the catalytic substrate.<sup>2</sup>

The use of SECM for the study and design of electrocatalysts is of ongoing interest in our group,<sup>8–13</sup> which also includes the electrochemical oxidation of formic acid.<sup>14</sup> This process has

- (1) *Scanning Electrochemical Microscopy*; Bard, A. J., Mirkin, M. V., Eds.; Marcel Dekker: New York, 2001.
- (2) Rodríguez-López, J.; Alpuche-Avilés, M. A.; Bard, A. J. *J. Am. Chem. Soc.* **2008**, *130*, 16985–16995.
- (3) Woods, R. Chemisorption at Electrodes. In *Electroanalytical Chemistry*; Bard, A. J., Ed.; Marcel Dekker: New York, 1976; pp 1–162.
- (4) Bard, A. J.; Fan, F. F.; Pierce, D. T.; Unwin, P. R.; Wipf, D. O.; Zhou, F. *Science* **1991**, *254* (5028), 68–74.
- (5) Bard, A. J.; Denuault, G.; Lee, C.; Mandler, D.; Wipf, D. O. *Acc. Chem. Res.* **1990**, *23*, 357–363.
- (6) Pust, S. E.; Maier, W.; Wittstock, G. Z. *Phys. Chem.* **2008**, *222*, 1463–1517.

- (7) Bard, A. J.; Faulkner, L. R. *Electrochemical Methods*; Wiley: New York, 2001.
- (8) Fernandez, J. L.; Walsh, D. A.; Bard, A. J. *J. Am. Chem. Soc.* **2005**, *127*, 357–365.
- (9) Sánchez-Sánchez, C. M.; Rodríguez-López, J.; Bard, A. J. *Anal. Chem.* **2008**, *80*, 3254–3260.
- (10) Minguzzi, A.; Alpuche-Avilés, M. A.; Rodríguez-López, J.; Rondinini, S.; Bard, A. J. *Anal. Chem.* **2008**, *80*, 4055–4064.
- (11) Lin, C.-L.; Sánchez-Sánchez, C. M.; Bard, A. J. *J. Electrochem. Solid-State Lett.* **2008**, *11*, B136–B139.
- (12) Lee, J.; Ye, H.; Pan, S.; Bard, A. J. *Anal. Chem.* **2008**, *80*, 7445–7450.
- (13) Sun, Y. M.; Alpuche-Avilés, M. A.; Bard, A. J.; Zhou, J. P.; White, J. M. *J. Nanosci. Nanotechnol.* **2009**, *9*, 1281–1286.

been widely studied in noble metals because of the potential use of HCOOH for fuel cells.<sup>15</sup> One of the limiting factors for the efficient electrochemical conversion of HCOOH to CO<sub>2</sub> and H<sup>+</sup> at Pt in acidic media is the poisoning and blocking effect of adsorbed intermediates,<sup>16,17</sup> such as CO<sub>ads</sub>, HCOO<sub>ads</sub> (“formate”), COH<sub>ads</sub>, COH<sub>ads</sub>, and HCO<sub>ads</sub>.<sup>18</sup> This has been investigated by the use of in situ IR and related methods, which are especially well suited for the detection of carbonyl species.<sup>18–22</sup> In early studies,<sup>23–25</sup> a route termed the “direct pathway”,<sup>19,26</sup> i.e., direct oxidation to CO<sub>2</sub> and H<sup>+</sup>, was identified as beneficial in terms of avoiding poisoning species. However, the “indirect pathway” (which generates CO<sub>ads</sub>) inevitably also comes into play.<sup>17</sup>

An important part of the discussion in the same early studies of HCOOH oxidation is the formation of H<sub>ads</sub> by the catalytic decomposition of HCOOH at the Pt surface (a leading route to the “direct pathway”); this discussion was fed by the observation that the open circuit potential (OCP) of a Pt electrode in contact with solutions of different concentrations of HCOOH would exhibit a transient that stabilized to potentials where H<sub>ads</sub> UPD is possible.<sup>23–25,27–31</sup> The quantification of this adsorbed species and how it related to such changes in the OCP were not fully described,<sup>30</sup> although recently these OCP measurements have come back into focus because of the interplay that adsorbed and solution-phase species have in HCOOH-based catalytic systems:<sup>32,33</sup> e.g., in electrochemical oscillators.<sup>22,34</sup>

The decomposition of HCOOH to CO<sub>2</sub> and H<sub>2</sub> is thermodynamically favored ( $\Delta G^\circ = -14$  kcal/mol),<sup>35</sup> and it has been well established in gas-phase studies that these are the main products on Pt surfaces,<sup>36–40</sup> especially at low temperatures

(reminiscent of low electrochemical overpotentials); in fact, other noble metals such as Pd are well-known to catalyze this decomposition,<sup>40–43</sup> a possible lead that links good electrocatalytic behavior, as it is with Pd and modified Pd electrodes, to gas-phase catalytic activity.<sup>14,15,25</sup> The role of HCOOH as a reducing agent in conjunction with Pt surfaces and colloids has been reported,<sup>44–46</sup> and recent computational studies have discussed the formation of H<sub>ads</sub> on Pt from HCOOH,<sup>47</sup> therefore, the quantification of this species by SI-SECM is clearly of interest. While the detection and quantification of this adsorbate through spectroscopic techniques remains elusive,<sup>48–50</sup> we hope that this in situ electrochemical approach is useful for the characterization of H<sub>ads</sub> (or other oxidizable species) on catalysts and electrocatalysts.

## Mode of Operation

Figure 1 shows the mode of operation of SI-SECM for the formation and quantification of H<sub>ads</sub>. The adsorbate is shown to be formed at a Pt electrode by either of two routes: the electrochemical underpotential deposition (UPD) of hydrogen adatoms achieved by applying a reduction potential to the Pt electrode (Figure 1A) or the catalytic decomposition of a substance, e.g., HCOOH through one possible pathway, at the Pt surface when the electrode rests at open circuit (Figure 1B). The first represents an electrocatalytic route and the second a catalytic route. Prior to either of these processes, an SECM interrogator electrode, e.g., a Au tip or glassy carbon electrode, is located concentrically to the Pt electrode a short distance from it ( $\sim 0.1\text{--}0.2 \times a$ , where  $a$  is the radius of the interrogator electrode). A reversible redox mediator, R, present in the solution, is oxidized to O at the interrogator electrode (Figure 1C); this oxidized mediator diffuses to the Pt substrate which is at OC. Species O reacts with H<sub>ads</sub> at the Pt surface to regenerate R. As depicted in Figure 1D, in the absence of H<sub>ads</sub> (the blank) the interrogator electrode would show the response labeled as negative feedback (NF): i.e., a geometric blocking of the diffusion of R. In the presence of H<sub>ads</sub>, the reaction of O and H<sub>ads</sub> to give R produces a transient larger current at the interrogator electrode for as long as H<sub>ads</sub> is available for reaction. This increased current is due to the transient collection of the regenerated R and gives quantitative information about the amount of H<sub>ads</sub> at the Pt surface by simple integration of the NF-background-subtracted signal. If the reaction between O and H<sub>ads</sub> is rapid and mechanistically uncomplicated, the path shown by the transient response follows that exhibited by a positive-feedback (PF) process, in which the Pt substrate regenerates R electrochemically by choice of a suitable potential bias.<sup>1,2</sup>

- (14) Jung, C.; Sánchez-Sánchez, C. M.; Lin, C.-L.; Rodríguez-López, J.; Bard, A. J. *Anal. Chem.* **2009**, *81*, 7003–7008.
- (15) Rice, C.; Ha, S.; Masel, R. I.; Wieckowski, A. *J. Power Sources* **2003**, *115*, 229–235.
- (16) Rodríguez, J. L.; Pastor, E. *Electrochim. Acta* **1998**, *44*, 1173–1179.
- (17) Lu, G.-Q.; Crown, A.; Wieckowski, A. *J. Phys. Chem. B* **1999**, *103*, 9700–9711.
- (18) Chen, Y.-X.; Shen, Y.; Heinen, M.; Jusys, Z.; Osawa, M.; Behm, R. J. *J. Phys. Chem. B* **2006**, *110*, 9534–9544.
- (19) Chen, Y.-X.; Heinen, M.; Jusys, Z.; Behm, R. J. *Langmuir* **2006**, *22*, 10399–10408.
- (20) Chen, Y.-X.; Heinen, M.; Jusys, Z.; Behm, R. J. *Chem. Phys. Chem.* **2007**, *8*, 380–385.
- (21) Miki, A.; Ye, S.; Senzaki, T.; Osawa, M. *J. Electroanal. Chem.* **2004**, *563*, 23–31.
- (22) Samjeske, G.; Miki, S.; Ye, A.; Yamakata, Y.; Mukouyama, H.; Okamoto, H.; Osawa, M. *J. Phys. Chem. B* **2005**, *109*, 23509–23516.
- (23) Breiter, M. W. *J. Electrochem. Soc.* **1964**, *111*, 1298–1299.
- (24) Gottlieb, M. H. *J. Electrochem. Soc.* **1964**, *111*, 465–472.
- (25) Munson, R. A. *J. Electrochem. Soc.* **1964**, *111*, 372–376.
- (26) Parsons, R.; VanderNoot, T. *J. Electroanal. Chem.* **1988**, *257*, 9–45.
- (27) Oxley, J. E.; Johnson, G. K.; Buzalski, B. T. *Electrochim. Acta* **1964**, *9*, 897–910.
- (28) Schwabe, K. *Z. Elektrochem.* **1957**, *61*, 744–752.
- (29) Breiter, M. W. *Electrochim. Acta* **1963**, *8*, 447–456, 457–470.
- (30) Fleischmann, C. W.; Johnson, G. K.; Kuhn, A. T. *J. Electrochem. Soc.* **1964**, *111*, 602–605.
- (31) Eckert, J. *Electrochim. Acta* **1967**, *12*, 307–328.
- (32) Podlovchenko, B. I.; Manzhos, R. A.; Maksimov, Y. M. *Russ. J. Electrochem.* **2006**, *42*, 1061–1066. See also: Podlovchenko, B. I.; Manzhos, R. A.; Maksimov, Y. M. *Russ. J. Electrochem.* **2006**, *42*, 658–664.
- (33) Podlovchenko, B. I.; Manzhos, R. A.; Maksimov, Y. M. *Electrochim. Acta* **2005**, *50*, 4807–4813.
- (34) Tian, M.; Conway, B. E. *J. Electroanal. Chem.* **2008**, *616*, 45–56.
- (35) Papapolymerou, G. A.; Schmidt, L. D. *Langmuir* **1987**, *3*, 1098–1102.
- (36) Columbia, M. R.; Thiel, P. A. *J. Electroanal. Chem.* **1994**, *369*, 1–14.
- (37) Columbia, M. R.; Crabtree, A. M.; Thiel, P. A. *J. Electroanal. Chem.* **1993**, *345*, 93–105.
- (38) Dahlberg, S. C.; Fisk, G. A.; Rye, R. R. *J. Catal.* **1975**, *36*, 224–234.

- (39) Tevault, D. E.; Lin, M. C.; Umstead, M. E.; Smardzewski, R. R. *Int. J. Chem. Kinet.* **1979**, *11*, 445–449.
- (40) Thomas, F. S.; Masel, R. I. *Surf. Sci.* **2004**, *573*, 169–175.
- (41) Baldauf, M.; Kolb, D. M. *J. Phys. Chem.* **1996**, *100*, 11375–11381.
- (42) Brandt, K.; Steinhilber, M.; Wandelt, K. *J. Electroanal. Chem.* **2008**, *616*, 27–37.
- (43) Burke, L. D.; Casey, J. K. *J. Appl. Electrochem.* **1993**, *23*, 573–582.
- (44) Burke, L. D.; Kemball, C.; Lewis, F. A. *Catalysis* **1966**, *5*, 539–542.
- (45) Ananiev, A. V.; Broudic, J.-C.; Brossard, P. *App. Catal., B* **2003**, *45*, 197–203.
- (46) Parravano, G. *J. Am. Chem. Soc.* **1950**, *72*, 5546–5549.
- (47) Bickford, D. F.; Coleman, C. J.; Hsu, C. L. W.; Eibling, R. E. *Ceram. Trans.* **1991**, *23*, 283–294.
- (48) Yue, C. M. Y.; Lim, K. W. *Catal. Lett.* **2009**, *128*, 221–226.
- (49) Hamada, I.; Yoshitada, M. *J. Phys. Chem. C* **2008**, *112*, 10889–10898.
- (50) Kunimatsu, K.; Senzaki, T.; Tsushima, M.; Osawa, M. *Chem. Phys. Lett.* **2005**, *401*, 451–454.
- (51) Chun, J. H.; Ra, K. H.; Kim, N. Y. *Int. J. Hydrogen Energy* **2001**, *26*, 941–948.

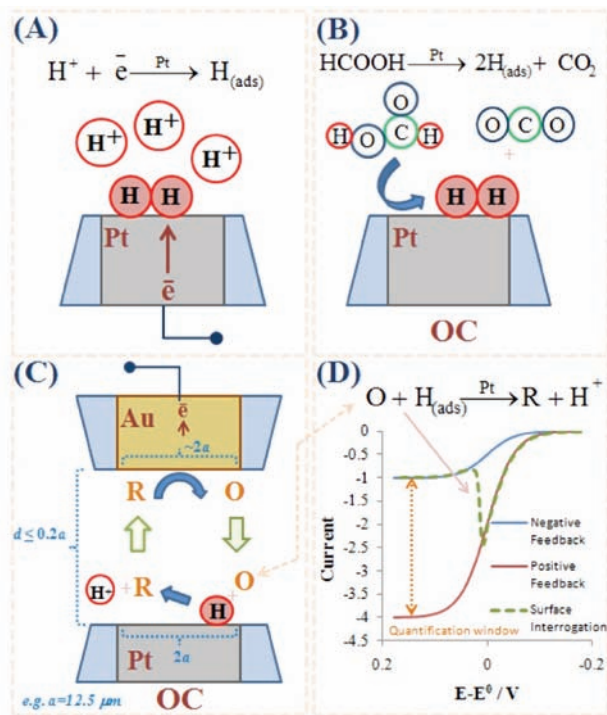


**Figure 1.** Depiction of the mode of operation of the surface interrogation technique for the oxidation of adsorbed hydrogen on Pt. (A) formation of  $H_{\text{ads}}$  by electrochemical UPD of H on Pt; (B) formation of  $H_{\text{ads}}$  by a possible catalytic decomposition pathway of HCOOH on the Pt substrate at open circuit; (C) interrogation of  $H_{\text{ads}}$  on a Pt substrate by an oxidized species O electrogenerated at an inert electrode (e.g., Au) from R (initially present in the solution) (Pt substrate is at open circuit; dimensions of the setup are exemplified using setup 1 described in the Experimental Section). (D) Depiction of SI results in the CV mode for the events in (C); reaction of O and  $H_{\text{ads}}$  takes place until all  $H_{\text{ads}}$  is consumed, and the transient follows the path exhibited by a positive feedback (substrate bias) scan of the O/R couple and then drops to the path exhibited by a negative feedback (no substrate bias) scan of the same couple.

## Experimental Section

**Chemicals.** All solutions were prepared with deionized Milli-Q water. Chemicals used as received were as follows: sulfuric acid (94%–98%) and perchloric acid (67%–71%), both trace metal grade, from Fisher Scientific (Canada); agar purified grade from Fisher Scientific (Fair Lawn, NJ); sodium acetate trihydrate and acetic acid glacial from Mallinckrodt (Paris, KY); silver nitrate (99+%), silver wire (99.9%), and sodium perchlorate (99%) from Aldrich (Milwaukee, WI); formic acid (96%) from Acros Organics (NJ); *N,N,N',N'*-tetramethyl-*p*-phenylenediamine (TMPD, 99%) from Sigma (St. Louis, MO); ferrocenemethanol (FcMeOH, 97%) from Aldrich (Russia); potassium hexacyanoruthenate(II) ( $K_4\text{Ru}(\text{CN})_6$ ), potassium hexachloroiridate(III) ( $K_3\text{IrCl}_6$ ), and tris(1,10-phenanthroline)iron(II) perchlorate ( $\text{Fe}(\text{phen})_3(\text{ClO}_4)_2$ ) from Alfa Aesar (Ward Hill, MA); ferrocenemono-carboxylic acid (FcCOOH, 97%) from Strem Chemicals (Newburyport, MA); carbon monoxide (CO) gas research grade from Specialty Chemical Products (South Houston, TX); hydrogen ( $\text{H}_2$ ) gas ultrahigh purity and argon gas from Praxair (Danbury, CT). Tris(2,2'-bipyridine)ruthenium(II) perchlorate ( $\text{Ru}(\text{bpy})_3(\text{ClO}_4)_2$ ) was prepared by metathesis of tris(2,2'-bipyridine)ruthenium(II) chloride ( $\text{Ru}(\text{bpy})_3\text{Cl}_2$ ) from GFS Chemicals (Columbus, OH) with sodium perchlorate in aqueous solution. Acetate buffer solution (pH 4, 0.1 M in acetate) was prepared by dissolving sodium acetate in water and adjusting the pH with acetic acid.

**Electrodes.** Gold (99.99+%) and platinum (99.99%) 25  $\mu\text{m}$  diameter wire and platinum (99.99%) and palladium (99.99%) 100

$\mu\text{m}$  diameter wire from Goodfellow (Devon, PA) were used to fabricate the SECM electrodes by procedures described elsewhere;<sup>1</sup> the tips used in this study had  $\text{RG} \leq 2$  (where  $\text{RG} = r_g/a$  and  $r_g$  is the radius of the tip's flat apex). Glassy carbon (GC) plates of 1 mm thickness from Alfa Aesar (Ward Hill, MA) were cut into squares of 1  $\text{cm}^2$  and selectively insulated with a PTFE dispersion precursor (Aldrich) through a previously reported procedure<sup>51</sup> to reveal a single GC microelectrode 200  $\mu\text{m}$  in diameter. All metallic electrodes were polished prior to use with alumina paste (0.05  $\mu\text{m}$ ) on microcloth pads (Buehler, Lake Bluff, IL), and sonicated for 15 min in water. Pt electrodes were further cycled between  $-0.1$  and 1.2 V versus NHE in 0.5 M sulfuric or 1 M perchloric acid to a constant CV previous to adsorption measurements.

Two electrode setups were used for the SI technique. In both cases, we will consider the Pt electrode as the substrate, whereas the other electrode, either Au or GC, is the interrogator electrode. Setup 1 consisted of a 25  $\mu\text{m}$  diameter Au interrogator electrode concentrically aligned to a 25  $\mu\text{m}$  diameter Pt substrate electrode and set 1–3  $\mu\text{m}$  apart in the  $z$  direction (corresponding roughly to 0.1–0.2 times the tip radius,  $a$ , as depicted in Figure 1C). Setup 2 consisted of a 200  $\mu\text{m}$  diameter GC interrogator electrode (from a selectively insulated GC plate) over which a 100  $\mu\text{m}$  diameter Pt substrate electrode was positioned and concentrically aligned at a 5–10  $\mu\text{m}$  distance in the  $z$  direction. These two electrode arrangements are equally valid for the purpose of the surface interrogation technique; the geometry in system 2 introduced in this study presents the same characteristics as described in ref 2, an important one being that any assembly that provides an adequate thin-layer cell (between the substrate and interrogator electrodes)<sup>7</sup> is useful, thus expanding the uses of the SI mode to materials where UMEs are difficult to fabricate. The procedure to align and approach the electrodes consists of the use of feedback and generation–collection SECM modes and has been discussed in detail in ref 2. In all experiments, an Ag/AgCl (saturated KCl, 0.197 V vs NHE) reference electrode was used; however, all potential measurements are reported versus NHE. Chloride leakage from this reference was prevented by the use of a 0.2 M sodium perchlorate/3% w/v agar salt bridge. A 0.5 mm diameter tungsten wire (Alfa Products, Danvers, MA) was used in all experiments as a counter electrode. All solutions used in the electrochemical cell were thoroughly bubbled with Ar prior to experimentation and were kept under a humidified argon blanket.

**Procedures.** SECM and other electrochemical measurements were done with either a CHI900 or CHI920C SECM station bipotentiostat (CH Instruments, Austin, TX). For studies on the behavior of mediators, the systems were tested in the feedback mode of SECM using setup 1. Once the electrodes were positioned, their positive and negative feedback characteristics were evaluated in the CV modality. Initially, only the reduced form, R, of the mediator is present in solution; its oxidized form, O, was produced at the interrogator electrode by scanning the potential from ca.  $-200$  mV to  $+200$  mV from the mediator  $E_{1/2}$  (in a microelectrode,  $E_{1/2}$  is the potential  $E$  when  $i/i_{\text{lim}} = 0.5$ , where  $i$  is the current and  $i_{\text{lim}}$  is the limiting current) at a scan rate,  $v$ , between 5 and 50 mV/s (slower scan rates are preferred for setup 2).<sup>7</sup> For positive feedback experiments, the Pt substrate was biased at a potential where reduction of O is possible: i.e.,  $-200$  mV from  $E_{1/2}$ . For negative feedback experiments, the Pt substrate was disconnected from the setup and allowed to rest at OC while the interrogator electrode was scanned.

For the evaluation of electrochemically generated UPD  $H_{\text{ads}}$  by the SI mode, the Pt substrate was scanned at 50 mV/s to potentials between 0.42 and 0.02 V vs NHE, stopping at different values of  $E$  between these bounds in order to dose different amounts of  $H_{\text{ads}}$ . Following this, the Pt substrate was brought to OC and the interrogator electrode (which was allowed previously to rest at OC)

(51) Rodríguez-López, J.; Alpuche-Aviles, M. A.; Bard, A. J. *Anal. Chem.* **2008**, *80*, 1813–1818.

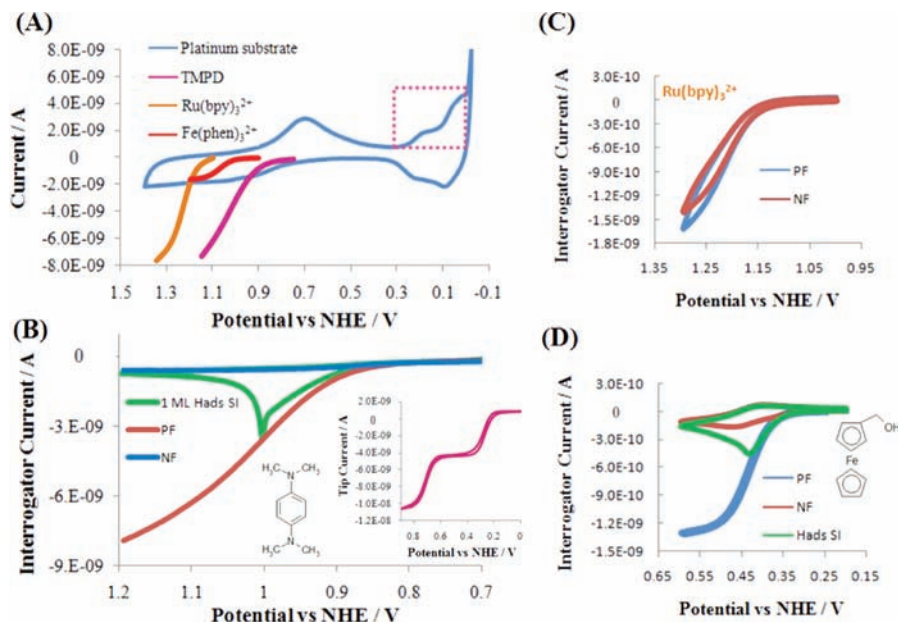


**Figure 2.** Behavior of different mediator systems for the SI mode ((A)–(C)) in Ar-purged 0.5 M H<sub>2</sub>SO<sub>4</sub>, (D) in Ar-purged 0.1 M acetate buffer pH 4). All NF scans were taken with the substrate at open circuit. All PF scans were taken with  $E_{\text{sub}}$  at least 0.3 V more negative than  $E_{1/2}$ . (A) CV of Pt UME ( $a = 12.5 \mu\text{m}$ ) at  $\nu = 50 \text{ mV/s}$  and comparison to positive feedback voltammograms of 0.5 mM mediator (TMPD, Ru(bpy)<sub>3</sub>(ClO<sub>4</sub>)<sub>2</sub> or Fe(phen)<sub>3</sub>(ClO<sub>4</sub>)<sub>2</sub>) on a Au UME ( $a = 12.5 \mu\text{m}$ ) at  $\nu = 50 \text{ mV/s}$  and  $d \approx 2.5 \mu\text{m}$  away from a Pt substrate UME ( $a = 12.5 \mu\text{m}$ ) (setup 1). (B) Surface interrogation of H<sub>ads</sub> at Pt with TMPD 0.5 mM (setup 1). H<sub>ads</sub> was dosed by taking the Pt substrate through a linear scan from 0.42 to 0.02 V at 50 mV/s. Interrogator electrode scan  $\nu = 20 \text{ mV/s}$ . Comparison was made to NF and PF for the same TMPD conditions. The inset shows the structure of TMPD and CV of TMPD in unbuffered 0.1 M K<sub>2</sub>SO<sub>4</sub>:  $\nu = 50 \text{ mV/s}$  at Au UME ( $a = 12.5 \mu\text{m}$ ). (C) Comparison of NF and PF scans for 0.1 mM Ru(bpy)<sub>3</sub>(ClO<sub>4</sub>)<sub>2</sub>,  $\nu = 20 \text{ mV/s}$ ,  $d \approx 2.5 \mu\text{m}$ . (D) Surface interrogation of H<sub>ads</sub> at Pt with FcMeOH (setup 1). H<sub>ads</sub> was dosed by taking the Pt substrate through CV from 0.2 to  $-0.24 \text{ V}$  at  $\nu = 200 \text{ mV/s}$ . Interrogator electrode scan  $\nu = 20 \text{ mV/s}$ . Comparison was made to NF and PF for the same FcMeOH conditions:  $\nu = 20 \text{ mV/s}$ . The inset shows the structure of FcMeOH.

was scanned (vide infra) to produce O from R. The feedback response of the interrogator electrode was recorded; the amount of interrogated adsorbate was obtained by subtracting the negative feedback background from the SI experimental results and integrating the result. These amounts were compared to the integration of the UPD H<sub>ads</sub> response obtained through a linear potential scan on the Pt substrate to the potential of 0.02 V vs NHE, charge to which is assigned a coverage of one monolayer (ML).

For the study of the decomposition of formic acid at the Pt substrate, setup 2 was used in all experiments. Prior to the addition of HCOOH to the electrochemical cell, the SI of 1 ML H<sub>ads</sub> UPD was obtained for comparison using TMPD as mediator. Into the well-deaerated solution containing 1 M HClO<sub>4</sub> and 0.5 mM TMPD, concentrated HCOOH was injected to give a final concentration of 12.5 mM. The OCP of the substrate was monitored with time, and at a desired value the interrogation was run by scanning the interrogator electrode to produce oxidized TMPD as described for SI of H<sub>ads</sub> UPD. At the end of each experimental session, a PF scan was run to verify that the alignment of the electrodes had not changed significantly throughout the experiments.

## Results and Discussion

**Choice of an Interrogation Mediator.** TMPD was found to be a good redox mediator for the interrogation of H<sub>ads</sub> at platinum at low pH, e.g., pH  $\sim 0$  in 0.5 M H<sub>2</sub>SO<sub>4</sub> or 1 M HClO<sub>4</sub>. The criteria used to determine the goodness of a mediator is largely based on the following characteristics: (1) high to moderate solubility in the medium, (2) stability of both forms of the redox pair, (3) a large difference in  $E^\circ$  with respect to adsorbed hydrogen ( $E^\circ = 0 \text{ V}$  vs NHE for the H<sup>+</sup>/H<sub>2</sub> pair, but preferably  $E^\circ > 0.4 \text{ V}$  for the mediator to be outside the UPD region on Pt), (4) low electrochemical background when performing the SI technique (which reflects lack of interaction

with the Pt substrate during the negative feedback acquisition), and (5) quantitative reaction of the oxidized form with H<sub>ads</sub>.

Figure 2A shows the cyclic voltammogram of Pt in 0.5 M H<sub>2</sub>SO<sub>4</sub> as well as the position of the oxidation waves for three mediators (0.5 mM each and shown in the PF mode using setup 1 that comply well with criteria 1–3): Ru(bpy)<sub>3</sub><sup>2+</sup> and Fe(phen)<sub>3</sub><sup>2+</sup>, which are metal complexes, and TMPD, an aromatic amine. These initial substances represent R in the previous discussion; their oxidation products, O, are good oxidizing agents that energetically overlap (to different degrees) in the region where the formation of oxides is observed in the CV of Pt. Only TMPD complies well with criteria 4 and 5, as is shown in Figure 2B. Working in the SI mode with TMPD and dosing the Pt substrate with H<sub>ads</sub>, this mediator is able to interrogate it quantitatively (recovery of H<sub>ads</sub> is greater than 97% for 1 ML of H<sub>ads</sub>); the SI response lies well within the interrogation window, as depicted in Figure 1D, and the negative feedback response shows a low background, roughly  $0.3i_{T,\infty}$ , where  $i_{T,\infty}$  represents the tip limiting current far away from the substrate; this level of background is expected for a well-behaved mediator under the conditions described in setup 1.<sup>2,52</sup> Figure 2B also reveals, however, that the SI response is shifted slightly from the trace drawn by the positive feedback scan and exhibits a sharp peak well into the interrogation wave. The oxidation of TMPD is pH sensitive; for instance, in unbuffered 0.1 M K<sub>2</sub>SO<sub>4</sub> (pH  $\sim 9$ ) the UME CV reveals two distinct waves at 0.28 and 0.72 V vs NHE of the same height ( $D_{\text{TMPD}} = 1.03 \times 10^{-9} \text{ m}^2/\text{s}$ ), suggesting two consecutive oxidation processes, as shown in the inset of Figure 2B. Under the acidic conditions of this study, we observe only one broad wave whose limiting

(52) Xiong, H.; Guo, J.; Amemiya, S. *Anal. Chem.* **2007**, *79*, 2735–2744.

current corresponds to a one-electron process in comparison to the unbuffered case. The need to apply a larger oxidation potential to drive the reaction may be indicative that oxidation is actually carried out on the protonated state of the TMPD molecule: i.e., it is harder to remove an electron from the positively charged TMPD molecule. Titration of a solution of TMPD with perchloric acid shows at least one protonation event, with  $pK_a = 6.3$  for the dissociation of  $\text{TMPDH}^+$  (Supporting Information, Figure S1), showing that indeed at the much lower pH in our experiments, TMPD participates as the protonated form. The shift of the SI response from the ideal PF response may be due to changes in the local pH environment brought about by the discharge of protons into solution as a consequence of the interrogation process, especially in the vicinity of the substrate, which may affect both the energetics and reaction kinetics of oxidized TMPD and  $\text{H}_{\text{ads}}$  in a more complex fashion than we have treated it so far. A detailed study on these effects is planned as more examples of SI systems are tested.

While TMPD was an adequate mediator for the interrogation of  $\text{H}_{\text{ads}}$  on Pt, other mediators based on metal complexes displayed a less satisfactory behavior. Figure 2C shows the comparison of the NF and PF scans upon oxidation of 0.1 mM  $\text{Ru}(\text{bpy})_3^{2+}$  in proximity to a Pt substrate in setup 1; the quantification window, as depicted in Figure 1D and as obtained for TMPD (Figure 2B), is almost absent. In the case of Figure 2C, the NF response exhibits an increased background that reaches the response level of PF; such a background is unacceptable for the quantification of  $\text{H}_{\text{ads}}$ . Upon interrogation of  $\text{H}_{\text{ads}}$ , the recovery was poor and often irreproducible. The large background observed in the NF scans can be rationalized in terms of the oxidized mediator O attacking the metal substrate to a small extent; in the case of platinum this could proceed through the formation of platinum oxides (PtOH, PtO) along with the regeneration of R, which could account for the recycling of the reduced species to give a positive feedback-like response where otherwise a low background should be observed. In fact, the use of oxidizing mediators in SECM studies has been applied extensively for the patterning and dissolution of substrates such as copper,<sup>53</sup> silver<sup>54</sup> and silver nanoparticles,<sup>55</sup> and semiconductors.<sup>56</sup> That the oxidation waves of mediators such as  $\text{Ru}(\text{bpy})_3^{2+}$  and  $\text{Fe}(\text{phen})_3^{2+}$  overlap the oxygen adsorption features in the Pt voltammogram, Figure 2A, allows for the possibility of them interacting to form Pt oxides. In this respect TMPD was a special case that did not follow this trend; thus, it allows for the study of a wide potential range on the Pt substrate ( $\sim 0$ –0.8 V vs NHE), which is optimal for the study of  $\text{H}_{\text{ads}}$ . The interrogation of  $\text{H}_{\text{ads}}$  on Pt was also studied at other pH conditions where more mediators are stable. Figure 2D shows the interrogation of  $\text{H}_{\text{ads}}$  at pH 4 in acetate buffer using ferrocenemethanol (FcMeOH) as mediator. While it was possible to establish a reasonably wide quantification window, recoveries with this mediator were about 90% and the reaction kinetics between O and  $\text{H}_{\text{ads}}$  were sluggish, as evidenced by the broad and slow decay of the SI scan in Figure 2D. FcMeOH, however, has the advantage of being oxidized at a potential that lies well in the double-layer region of Pt at this pH, and this is probably the

reason the NF scans show a moderately low background, unlike more oxidizing mediators (Supporting Information, Figure S2). Notably, other types of oxidizing mediators, such as  $\text{Br}_2$ , produced from the electro-oxidation of  $\text{Br}^-$ , provided low backgrounds on NF, which may be linked to the suppression of oxide formation on the Pt substrate; this case has been explored concurrently with the present study by demonstration of the reactivity of electrogenerated  $\text{Br}_2$  and adsorbed CO on Pt.<sup>57</sup>

**Surface Interrogation at Different  $\text{H}_{\text{ads}}$  Coverage on Pt.** The quantitative surface interrogation of  $\text{H}_{\text{ads}}$  on Pt by TMPD in acidic media was studied with different amounts of  $\text{H}_{\text{ads}}$  dosed to the substrate electrode. Figure 3A shows a typical progression of SI scans performed by a GC interrogator electrode (setup 2) on a Pt substrate dosed with  $\text{H}_{\text{ads}}$ ; the amount of  $\text{H}_{\text{ads}}$  was adjusted by scanning the substrate to different potentials within the UPD region for hydrogen, as depicted in the inset by the dashed lines. A common feature exhibited by these SI scans was a displacement of the peak signal with respect to the dosage. This displacement is related to the shift observed in Figure 2B with respect to the PF scans, which we have discussed in terms of the pH-sensitive nature of TMPD and the discharge of protons after the interrogation process. The SI scans do follow a common trace that ends in a sharp peak, whose integration yields  $\sim 2\%$  of a monolayer of  $\text{H}_{\text{ads}}$ . At lower doses, however, e.g., a potential limit of 0.32 V, the SI features are less shifted from the PF scan, thus suggesting that pH effects may have a lesser contribution to the shape of the SI scans. A better measure of the goodness of the SI scans lies in the quantitative comparison of  $\text{H}_{\text{ads}}$  found by SI vs the amount dosed (determined by integration of the charge delivered during the linear sweeps on the substrate). Figure 3B shows such a comparison for a series of experiments performed on both setups 1 and 2. There is quantitative agreement to approximately 0.2 V more positive than the onset of hydrogen evolution, with an average standard deviation of 5% of a monolayer for five independent experiments. The disagreement observed for more positive potentials in Figure 3B, which accounts roughly for 10% of a monolayer of  $\text{H}_{\text{ads}}$ , was further investigated. The inset of Figure 3B shows two SI experiments conducted by taking the substrate to 0.42 V in the presence of traces of  $\text{O}_2$  (typical experimental Ar-purging conditions) and upon even more extensive purging with Ar and its comparison to a NF scan; the results suggest that there is a link between the feature observed at these potentials and a non-negligible oxygen reduction process, possibly indicative of an adsorbed intermediate derived from this reaction. This peak is only observed upon substrate bias, which is the reason it is still possible to obtain good NF scans. Note, however, that the extensive purging conditions used to prove this point are impractical enough to prevent us from maintaining them over long periods of time and, thus, are not achievable under our typical experimental conditions in our SECM cells.

The possible contribution of TMPD adsorption at the Pt substrate to the observed discrepancy was evaluated by comparison of the voltammograms of  $\text{H}_{\text{ads}}$  UPD in the presence and absence of TMPD and by chronocoulometry of TMPD oxidation (Figure S3, Supporting Information), showing from 0.4% to 4.6% ML adsorption, which lies well within the measured standard deviation of 5%. Adsorption of the protonated TMPD, as in our experiments, seems unlikely in view of its increased hydrophilicity compared to the free base TMPD; its contribution to any measurable signal is very

(53) Macpherson, J. V.; Slevin, C. J.; Unwin, P. R. *J. Chem. Soc. Faraday Trans.* **1996**, *92*, 3799–3805.

(54) Zhang, M.; Bin, S.; Cortes-Salazar, F.; Hojeij, M.; Girault, H. H. *Electrochem. Commun.* **2008**, *10*, 714–718.

(55) Schnippering, M.; Powell, H. V.; Zhang, M.; Macpherson, J. V.; Unwin, P. R.; Mazurenka, M.; Mackenzie, S. R. *J. Phys. Chem. C* **2008**, *112*, 15274–15280.

(56) Sheffer, M.; Mandler, D. *J. Electrochem. Soc.* **2008**, *155*, D203–D208.

(57) Wang, Q.; Rodríguez-López, J.; Bard, A. J. *J. Am. Chem. Soc.* **2009**, *131*, 17046–17047.

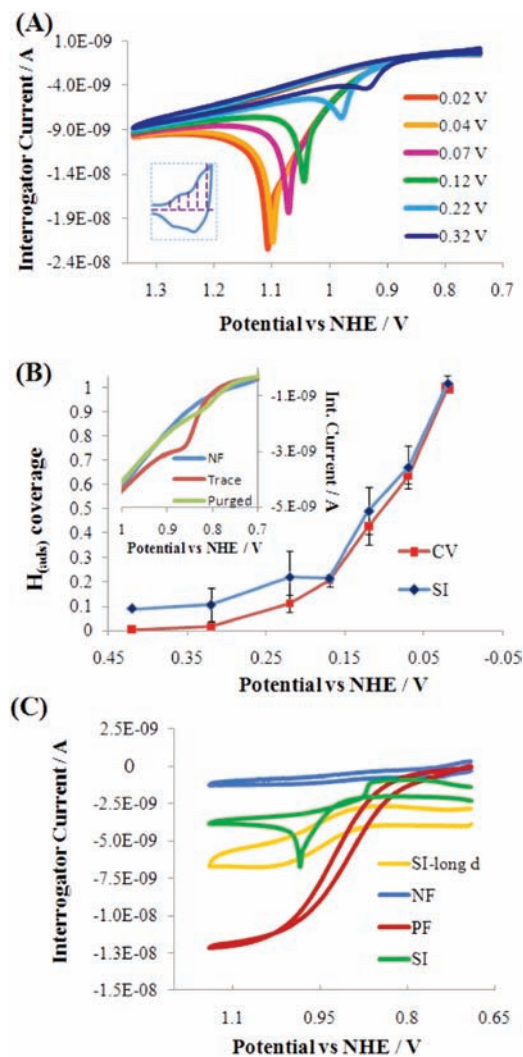


**Figure 3.** Surface interrogation of  $H_{\text{ads}}$  on Pt. (A) SI scans using 0.5 mM TMPD in 1 M  $\text{HClO}_4$  with different doses of  $H_{\text{ads}}$  delivered to the Pt substrate by a linear sweep at  $\nu = 50$  mV/s from 0.42 V to the potential limit indicated for each curve. Setup 2 was used, interrogator electrode  $\nu = 5$  mV/s. The inset shows representation of the potential limits on the Pt substrate sweep used during the  $H_{\text{ads}}$  dosage. (B) Comparison of the normalized charge from SI and sweep experiments (CV) at different corresponding potential limits of  $H_{\text{ads}}$  dosage. Normalization is done with respect to the hydrogen UPD integrated charge to a potential limit of 0.02 V on the sweep experiment at the substrate, which is assigned the value of 1 ML. Results from both setup 1 and setup 2 are averaged. The inset shows SI scans of the system when the potential limit of 0.42 V was used with trace oxygen (brown) and after extensive Ar purging (green) and the comparison to NF (blue); setup 2,  $\nu = 5$  mV/s. (C) Effect of addition of hydrogen gas to the system. The solution is 1 M  $\text{HClO}_4 + 0.5$  mM TMPD, and in the presence of  $H_2$ , it was added to saturation following Ar purging. Setup 1 is used and interrogator scan  $\nu = 20$  mV/s. A long-distance SI scan was done 15  $\mu\text{m}$  further away than the SI scan. NF in the absence of added  $H_2$ .

small, leaving most of the Pt surface available for  $H_{\text{ads}}$  adsorption. The described 10% discrepancy is an interesting finding; however, further exploration will be conducted separately from this study. An important message remains that trace background processes may play an important role in the quantification and assignment of the signals observed in SI scans. Furthermore, the effects of interfering species such as  $O_2$  itself will be shown to be relevant in the following discussion about the decomposition of HCOOH on Pt.

An experiment in the presence of dissolved  $H_2$  gas in acidic solution was carried out (setup 1) as shown in Figure 3C. In the SI configuration, the interrogator electrode response shows a peak with characteristics similar to those described for limiting  $H_{\text{ads}}$  dosing, Figure 3A; this peak is not observed when the SI scan is taken at a greater distance from the substrate, which confirms the surface nature of the  $H_2$  adsorption process. A constant background offset with respect to the NF level is also observed in Figure 3C. This offset is probably due to the supported oxidation of  $H_2$  by the mediator at the Pt surface, which suggests a continuous and fast formation of  $H_{\text{ads}}$  at Pt from this precursor. This type of effect is expected for those catalytic systems in which the parent molecule decomposes quickly at the substrate. The following sections deal with the decomposition of HCOOH at Pt, a process which is slow enough so that this background effect is absent and can be neglected. Note, however, that the possibility of using a mediator to carry out an inner-sphere reaction supported at a suitable catalyst (in this case Pt catalyzing the decomposition of  $H_2$ ) and obtaining a feedback current from it may be an interesting way of studying mediated electrocatalysis through a heterogeneous catalyst.

**Detection of HCOOH Decomposition on Pt.** We used the SI technique to show that formic acid is catalytically decomposed on a Pt surface at open circuit to produce  $H_{\text{ads}}$  and that the amount of this adsorbate is related to the open circuit potential (OCP) of the system at the time of interrogation. Figure 4A shows a typical open circuit transient measured in the presence of 12.5 mM formic acid in 1 M  $\text{HClO}_4$  and 0.5 mM TMPD for a Pt substrate assembled in setup 2 (in this setup a GC electrode is used as the interrogator, since this material is not active for the oxidation of HCOOH, while Au is reported to have some electrocatalytic activity).<sup>58</sup> In the absence of formic acid, the open circuit potential of the Pt substrate in this solution is typically close to the foot of the TMPD oxidation wave ( $\sim 0.7$  V); upon injection of HCOOH into the solution, the OCP of the platinum substrate dropped to a limiting potential of  $\sim 0.22$  V depending on the concentration of HCOOH (in  $t \approx 300$  s for this study where  $[\text{HCOOH}] = 12.5$  mM) and the amount of trace  $O_2$  in the electrochemical cell. The shape and potential limits of an OCP transient such as that shown in Figure 4A is consistent with that reported by others<sup>25,32,33</sup> and known since early studies of the decomposition of HCOOH.<sup>23–31</sup> This displacement of the OCP toward more negative potentials is an indicator of the formation of  $H_{\text{ads}}$ , although to our knowledge a clear quantification of such an intermediate is lacking, especially under the conditions of this study, where the Pt substrate is not biased. Figure 4A also shows for comparison that, in the two-electrode assembly, only the potential of the Pt substrate which catalyzes HCOOH decomposition changes with time, while the GC interrogator shows only a negligible drift. Note that the measurements here rely on the nondisturbance of the Pt substrate: i.e., the two-electrode SI setup is used to probe the catalytic activity of the metal, rather than its electrocatalytic behavior. The interrogator electrode probes the adsorbed species at the Pt surface through the use of the TMPD mediator, without the need for performing any amperometric or other dynamic measurements on the Pt electrode.

Figure 4B shows a set of SI scans where the substrate was interrogated after reaching different open circuit potential values in the presence of HCOOH. Qualitatively we note the similarities

(58) Zhang, Y.; Weaver, M. J. *Langmuir* **1993**, *9*, 1397–1403. Hamelin, A.; Ho, Y.; Chang, S.-C.; Gao, X.; Weaver, M. J. *Langmuir* **1992**, *8*, 975–981.

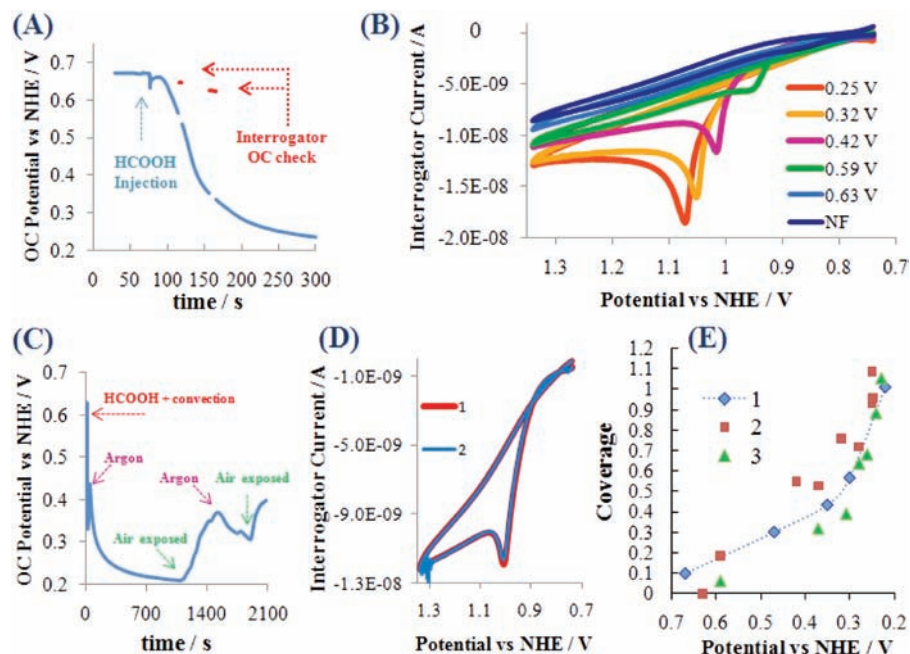


**Figure 4.** SI study of the decomposition of HCOOH on Pt. All solutions: 1 M HClO<sub>4</sub> + 0.5 mM TMPD + 12.5 mM HCOOH and Ar-purged to traces of O<sub>2</sub>. All experiments were done using setup 2. (A) Open circuit transient on the Pt substrate in the presence of HCOOH. Red traces show a switch to measurement of the interrogator electrode OCP. (B) Representative SI measurements at various OCP of the Pt substrate. Interrogator electrode  $\nu = 5$  mV/s. (C) OCP transient of Pt in the presence of HCOOH showing the effect of exposure to O<sub>2</sub> and its removal. (D) Reproducibility of SI measurements after OC variations as shown in (C). Scans 1 and 2 were obtained at a substrate OC potential of 0.3 V,  $\nu = 5$  mV/s. (E) H<sub>ads</sub> coverage vs OC potential as determined by three independent SI experiments. The blue dashed line on experiment 1 is added to guide the eye. One ML of H<sub>ads</sub> was determined from integration of the UPD region at the substrate on a linear potential scan prior to addition of HCOOH.

to the SI scans done for the interrogation of H<sub>ads</sub> from the UPD of hydrogen (Figure 3A); there is a shift of the peak intensity with respect to the interrogator potential at growing signal intensity. The amount of interrogated adsorbate was larger for less positive OCP of the substrate, reaching a limit when the OCP transient stabilized (Figure 4A). After an SI scan was performed on the substrate, its OCP was observed to restart from a positive value, e.g. 0.6–0.7 V, and the transient toward less positive potentials was reproduced; interrogation at different potentials could be carried out numerous times during an experiment, which suggests that the adsorbate can form reversibly on the Pt surface. An interesting effect was observed upon admission of air into the electrochemical cell; Figure 4C shows that when air is allowed into the solution, the OCP transient reverses toward more positive potentials, a possible indication that the adsorbed intermediate is removed by O<sub>2</sub>. When air was then removed by Ar purging, the potentials shifted again to less positive values. Parravano<sup>45</sup> observed that a Pt colloid in contact with HCOOH upon admission of O<sub>2</sub> led to the formation of an intermediate that initiated the polymerization of methyl methacrylate, but not in well-deaerated solutions, where possibly H<sub>ads</sub> is a less reactive species. Figure 4D shows an example of reproducible interrogation done at the same potential limit upon admission and removal of air in the cell in a cycle such as the one shown in Figure 4C; the interrogation scan retraced regardless of the path taken to arrive to the desired OCP.

Figure 4E shows the quantification of the adsorbate (normalized to 1 ML of UPD H<sub>ads</sub>) for three series of experiments; the most relevant experimental finding is the dependence of the adsorbate coverage with respect to the OCP of the Pt substrate at the time of interrogation. As shown in Figure 4A, the OCP transient reaches a limiting value near 0.22 V, which also coincides in limiting the amount with the charge corresponding

to 1 ML of UPD H<sub>ads</sub>; the potential window exhibited by Figure 4E is wide, and in fact the limiting potential of 0.22 V is barely within the UPD region of platinum, although the quantification of the adsorbate strongly suggests that it can be identified as H<sub>ads</sub>. Possible larger intermediates, such as physisorbed HCOOH,<sup>23</sup> formyl H•CO<sub>ads</sub>, “formate”-like species H•COO<sub>ads</sub>,<sup>22</sup> or even CO<sub>ads</sub><sup>59</sup> would occupy more than one H<sub>ads</sub> site, and hence a limiting coverage of 1 ML would less likely be attained, although some of these species cannot be discarded as possible intermediates. In the case of physisorbed HCOOH the slow establishment of the limiting conditions in an environment which is well in excess of this substance and the potential dependence of the interrogated signal (especially with respect to the presence of oxygen) makes us discard it as our quantified adsorbate; recent DFT calculations also suggest that HCOOH adsorbs only weakly at the Pt(100) crystal (the same for CO<sub>2</sub>, which we will only consider a nonadsorbed product).<sup>47</sup> The overall decomposition of HCOOH on Pt to yield a monolayer of H<sub>ads</sub> is estimated to be at least 500 times slower than the diffusion-limited rate of HCOOH arrival to the electrode (see the Supporting Information). We have assumed that this reaction is slow enough to neglect the effects of continuous decomposition of HCOOH during the SI scans, since the subtracted background from the SI experiments was run in the presence of HCOOH, e.g. when the OC of Pt is most positive (as in a consecutive scan after the main SI scan), and it shows no relevant difference from an NF scan (in the absence of HCOOH), as shown in Figure 4B. An estimation of the quantification error can be made, and corrected coverage values based on Figure 4B,E are shown in Figures S4 and S5 and Table S1 in the Supporting Information. The

(59) Offer, G. J.; Kucernak, A. R. *J. Electroanal. Chem.* **2008**, *613*, 171–185.

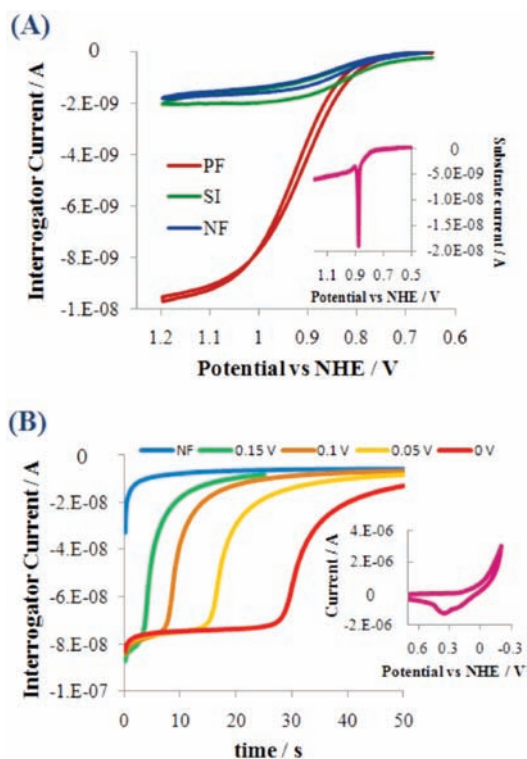


**Figure 5.** Additional SI experiments. (A) Effect of addition of CO gas to 1 M HClO<sub>4</sub> + 0.5 mM TMPD; CO added to saturation following Ar purging. Setup 1 is used, and interrogator scan  $\nu = 20$  mV/s. NF in the absence of added CO. The inset shows CO stripping at the Pt electrode after the SI scan,  $\nu = 100$  mV/s. (B) SI scan measurement on Pd dosed with adsorbed/adsorbed hydrogen. Setup 2 is used in the chronoamperometry mode;  $E_{\text{step}} = 1.15$  V for interrogator electrode. The Pd substrate was dosed by stepping for 3 s to selected potentials in 0.5 M H<sub>2</sub>SO<sub>4</sub> + 0.5 mM TMPD. The inset shows a CV of such a “bright” Pd electrode.

estimated error is lower the higher the measured coverage; at high coverages ( $E_{\text{OCP}} \approx 0.22$  V) this error is estimated to result in an overquantification of  $\sim 15\%$  ML, while at low measured coverages, the uncertainty between the beginning of interrogation and the duration of the interrogation process cancels out the low coverage found in the 0.7–0.45 V region.

The possibility that oxidized TMPD reacts with adsorbed carbon monoxide, CO<sub>ads</sub>, was also assessed, since this is a possible product or intermediate of the decomposition of HCOOH. Figure 5A shows an SI scan over a Pt substrate dosed with gaseous CO (no HCOOH) and its comparison to NF and PF; the TMPD system shows no response to this adsorbate, although its presence could be detected by conventional voltammetry on the Pt substrate (inset of Figure 5A). We conclude that the response obtained by the SI scans upon HCOOH decomposition does not come from adsorbed CO. Weak evidence that this species may be formed to some extent lies in the reproducibility of our measurements, especially in the high H<sub>ads</sub> coverage range (open circuit potentials 0.27–0.22 V). Over extended periods of experimentation time,  $\sim 2$ –3 h, quantifications found at the least positive potentials dropped up to 10%, which may be indicative of a loss in the activity of the Pt substrate due to accumulation of CO<sub>ads</sub>. Even in this scenario, our results contrast with the RAIRS measurements of Ma and Zaera,<sup>60</sup> in which exposure of Pt to HCOOH in neutral unbuffered media at open circuit provided a signal identified

as CO<sub>ads</sub> in presumably high coverages almost immediately; the question arises whether the pH or the concentration of HCOOH plays an important role in the formation of CO<sub>ads</sub>. Surface interrogation experiments at pH 4 (acetate buffer) and pH 7 (phosphate buffer) using FcMeOH (TMPD is not a satisfactory mediator at these pHs, see Figure 2B inset) as mediator reveal no time dependence of the OCP and no detectable SI feedback upon interrogation. At this pH, however, the predominant species is the formate anion (HCOO<sup>−</sup>) rather than HCOOH ( $pK_a = 3.74$ ), which significantly changes the nature of our measurements and discussion. We have recently developed the use of electrogenerated Br<sub>2</sub> for the quantification of CO<sub>ads</sub>,<sup>57</sup> and studies are under way for its quantification in electrocatalytic systems such as in the electrochemical oxidation of formic acid, methanol, and ethanol on Pt, where its participation as an intermediate is possibly of more importance than in the present study due to its *poisoning* effect. In the case of the electrochemical oxidation of HCOOH “formate”-like species and CO<sub>ads</sub> are said to form, even at low potentials, as observed through IR techniques<sup>18–22</sup> (despite certain discrepancies among these studies)<sup>21</sup> and predicted by some DFT calculations.<sup>61</sup> It remains an interesting and fundamental case how the described catalytic reaction of HCOOH on Pt reveals a slow but reversible route for the decomposition of this molecule to yield H<sub>ads</sub>, which as explained in the Introduction shows an interesting parallel to the gas/solid interface observations. Furthermore, the mechanism by which CO<sub>ads</sub> may be formed remains also an open question, whether it is a consequence of a parallel path in the decomposition of the “formate”-like species<sup>47</sup> or perhaps a slow inverse water-gas shift reaction between H<sub>ads</sub> and weakly bound CO<sub>2</sub> to generate water and CO.<sup>62</sup>

**Other Experiments: Hydrogen Interrogation on Pd.** Palladium is known to involve both adsorption and absorption (into the bulk metallic phase) of atomic hydrogen.<sup>40–43</sup> SI experiments with TMPD were conducted to evaluate the possibility of “titrating” this species by use of SI in the chronoamperometry mode<sup>2</sup> (where the mediator is produced by a potential step rather than a scan and is better suited for very large amounts of titrated material). Figure 5B shows an example of an experiment in which a bright Pd electrode was dosed with hydrogen at reducing potentials for 3 s in each case; the inset of the figure shows the CV of this type of electrode in acid media, which shows a poor electrochemical response for the oxidation of hydrogen species. The SI scans show a very clear and distinct titration response; we envision that our technique could be well suited for estimating the amounts of adsorbed hydrogen in confined Pd-based materials, such as thin layers.<sup>41</sup> In any case, we make the point that the SI technique can be used for a wider variety of materials and purposes than the main topic discussed in this work.

## Conclusions

The surface interrogation (SI) mode of scanning electrochemical microscopy (SECM) was shown to be a quantitative technique for the *in situ* quantification of adsorbed hydrogen, H<sub>ads</sub>, at polycrystalline platinum. This technique allowed us to decouple the measurement of this adsorbate from the action of the Pt substrate through the detection of a positive feedback loop on an interrogator electrode placed at a close distance from

(61) Neurock, M.; Janik, M.; Wieckowski, A. *Faraday Discuss.* **2008**, *140*, 363–378.

(62) Jacobs, G.; Patterson, P. M.; Graham, U. M.; Crawford, A. C.; Davis, B. H. *Int. J. Hydrogen Energy* **2005**, *30*, 1265–1276.

(60) Ma, Z.; Zaera, F. *Catal. Lett.* **2004**, *96*, 5–12.



the substrate, which remains at open circuit. The sensing mechanism is based on the production of an oxidized mediator at the interrogator electrode from a reversible redox species; this oxidized mediator can react with  $H_{ads}$  at the Pt substrate and regenerate the reduced form of the mediator, which is collected by the interrogator electrode as long as the oxidation reaction proceeds at the substrate.

TMPD was shown to be a satisfactory mediator for very acidic media, showing reversible and stable behavior while also presenting quantitative recovery of  $H_{ads}$  and low electrochemical background in the absence of the adsorbate. Metal complexes, however, exhibited a high electrochemical background, which is assumed to derive from their ability to oxidize the Pt substrate, rendering their interrogating capabilities untrustworthy. A less oxidizing mediator, FcMeOH, shows a reasonable behavior at higher pH (e.g., pH 4), where TMPD can no longer be used due to its pH-sensitive oxidation potential.

The quantification of  $H_{ads}$  was proved by interrogation of this adsorbate at different dosing levels on Pt achieved through UPD adsorption at the substrate. The SI quantifications agree well with the amounts dosed at high coverages, while they show a 10% of a monolayer of  $H_{ads}$  discrepancy at low coverages; this discrepancy was explained by the role that impurities of  $O_2$  can have on the Pt substrate upon potential bias. The decomposition of dissolved  $H_2$  by the Pt substrate and its interrogation showed that  $H_{ads}$ , in this case, the product of a catalytic reaction, could be probed.

The decomposition of formic acid on Pt, a slow catalytic reaction that has been assumed to produce  $H_{ads}$  in unclear amounts, was chosen as a model system to probe the quantification capabilities of the SI mode with TMPD as mediator. This reaction shows a transient decay of the open circuit potential of the Pt substrate; the use of the SI technique at different potential limits of the OCP at the Pt substrate revealed an

increasing amount of adsorbate until reaching both a potential and quantification limit at  $\sim 0.22$  V vs NHE, at which an amount close to 1 ML of  $H_{ads}$  was quantified. The quantification of the adsorbate depended on the OCP of the Pt substrate at the time of interrogation and was independent of the path taken to arrive at a given OCP value;  $O_2$  was shown to consume the adsorbate and displace the OCP of the substrate to more positive values. Such reversible behavior, along with the observed limiting coverage, the possibility of forming  $H_{ads}$  from HCOOH, and reports of this process in other systems such as the gas/metal interface, suggested the identification of the adsorbate as  $H_{ads}$ ; however, we cannot rule out the participation of other hydrogenated intermediates. TMPD was shown not to react with nor quantify  $CO_{ads}$ . Experimental possibilities with Pd are suggested.

**Acknowledgment.** We thank the National Science Foundation (No. CHE-0808927) and the Robert A. Welch Foundation (No. F-0021) for support of this research. J.R.-L. thanks Eli Lilly & Co. and the Division of Analytical Chemistry of the ACS for a DAC fellowship and also the complementary scholarship support provided by the Secretaría de Educación Pública of México and the Mexican Government.

**Note Added after ASAP Publication.** Due to a production error, the final paragraph of the Conclusions section in the version of this article published ASAP March 12, 2010, was from an earlier version of the manuscript. The redundant paragraph was deleted in the version published March 18, 2010.

**Supporting Information Available:** Text and figures giving additional experimental data. This material is available free of charge via the Internet at <http://pubs.acs.org>.

JA9090319